Proceedings of 12th Asian Congress of Fluid Mechanics (12ACFM)

ASIAN CONGRESS OF FLUID MECHANICS

17 ~ 21 August, 2008
Daejeon Convention Center
Daejeon, Korea

Click Here

T-2E-1. INFLUENCE OF TRAILING WALL ANGLE ON THE UNSTEADINESS OF CAVITY FLOWS
VIKRAMADITYA, N. S. *IIT MADRAS, India*, Job KURIAN, *IIT MADRAS, India*, An experimental study of supersonic flow over two-dimensional cavities is presented in this paper. All the experiments were carried out at uniform free stream Mach number of 1.63. The Reynolds number of the boundary layer at the leading edge of the cavity is found out to be 1.47548e+07. For constant length to depth ratio (L/D=3) trailing wall angle of cavity was varied. Experiments were performed on six different trailing wall angle cavities to understand its effect on the unsteadiness of cavity flows. A measurement of unsteady surface pressure at various locations inside the cavity was carried out. Standard statistical analysis methods have been used to obtain various quantities of interest including the spectral distributions. On the analysis of pressure signals, reduction in amplitudes of the modes was observed as the angle decreases to lower value. High magnitude oscillations were observed for 90 and 75 degrees cavities. Steep fall in amplitudes of oscillations was noticed as the angle is reduced below 75 degrees. Virtually no oscillation was observed for cavities with 30 and 15 cavities. Temporal mode switching was observed dependent on trailing wall angle of the cavity. Multiple modes exist as the trailing wall angle is reduced to a lower value. Existence of strong acoustic wave inside the cavity responsible for high amplitude oscillations in 90 and 75 degrees trailing wall angle cavities was detected. It is noticed that as the trailing wall angle was reduced below 75 degrees the feed back mechanism has weakened considerably. It is found that overall cavity behavior changes significantly as the trailing wall angle is reduced below 75 degrees.

T-2E-2. COMPUTATIONAL STUDY ON THE OPERATING PROCESSES OF A TWO-STAGE LIGHT-GAS GUN
G. RAJESH, *Department of Mechanical Engineering, College of Engineering, Trivandrum, Kerala, India*, H. D. KIM, *Andong National University, Korea*, Y. K. LEE, *Poongsan Company, Chungnam, Korea*, Two-stage light gas guns are commonly used to simulate projectile velocities in the ballistic regimes, and have been extensively been used in hyper-velocity impact engineering, supersonic and hypersonic projectile aerodynamics and aeroballistics. In general, the conventional two-stage light-gas gun consists of three tubes, two diaphragms, a piston and a projectile. The high-pressure tube serves as the reservoir of high-pressure gas. The pump tube, which contains a light-gas, to increase the speed of sound, is connected to the high-pressure tube through a diaphragm separating both at the junction. A massive, freely movable piston is placed near the diaphragm in the pump tube. Projectile is kept in the launch tube which is connected to the pump tube through another diaphragm. Rupture of the diaphragm between the high-pressure tube and pump tube causes the piston to move at a high-speed and isentropically compress the light-gas to a much higher pressure than that in the high-pressure tube. With this rapid rise of the pressure inside the pump tube, a state is reached at which the second diaphragm ruptures and shock tube flow is initiated with the production of a strong unsteady shock wave in the launch tube. Resulting high-pressure state just behind the projectile produced by the reflection of the shock wave from the projectile base, drives the projectile with a very high-velocity. The performance of such a two-stage light-gas gun can be determined by the projectile speed at a given pressure in the high-pressure tube and a given mass of the piston. In this case, the projectile speed is dependent on many other parameters such as, the kind of light-gas (driver gas), the length and diameter of each tube, the isentropic compression process due to the piston motion and the shock compression on the base of the projectile. A large number of the works have been carried out analyze the processes inside the two-stage light-gas gun. However, none of the works has focused on the complete simulation of the device, which is very much important in terms of the fluid dynamic and structural aspects of the device. In the present study, a CFD method has been applied to predict the compressible flow field inside the two-stage light-gas gun, and to find out the dependence of several operating parameters on the projectile velocity and the peak pressures in the device, aiming at the performance enhancement of the two-stage light-gas gun. The unsteady, compressible Euler equations were numerically solved using a fully implicit finite volume method. The chimera scheme was employed to simulate the moving piston in the pump tube and the motion of the projectile in the launch tube. The computational results are compared with experimental data and found to be in very good agreement. Based on the computational results, it is seen that the complete interior ballistics of such guns can be simulated using CFD method with reasonable accuracy.

T-2E-3. EXPERIMENTAL STUDY OF ACTIVE CONTROL IN TRANSONIC DIFFUSER
M. YAGA, *University of the Ryukyus, Japan*, Y. UECHI, *University of the Ryukyus, Japan*, S. MATSUDA, *Okinawa National College of Technology, Japan*, I. SENAHA , *University of the Ryukyus, Japan*, Preliminary experiments of an active control of shock waves and the pressure fluctuations in a transonic diffuser were carried out using a piezo actuator attached at a throat of the diffuser. The experiments were performed with a 0.7MPa blow down wind tunnel. The test section consists of a 500mm circular arc half nozzle and the piezo actuator set at the throat. The flow was measured with the high response semiconductor pressure sensors and observed with the high speed camera by mean of schlieren technique. As the input signals to the piezo actuator, the sinusoidal voltage of 100Hz and 200Hz were adopted. As expected, the shock wave in the diffuser has clear correlation with the piezo actuator, where the dominant frequency of the unsteady positions of the shock wave is exactly the same as the input frequency. It is also confirmed that the flow pattern and the shape of the shock wave remain unchanged under the different input frequencies. The time averaged shock positions increases with the wind tunnel pressure ratio, which means that the oscillating shock wave moves downstream monotonically with the increase in the wind tunnel pressure ratio. The rms (root mean square) of the wall static pressure ratio also provide us with the information on where and how the shock wave approaches to the five monitoring positions. It illustrated the clear peaks at different pressure ratios at each monitored position. These clear peaks are caused by the large pressure difference between downstream and upstream of the approaching shock wave. However, the results of detailed FFT analyses of the wall static pressure fluctuations under various pressure ratio show that for the input frequency of 100Hz the dominant frequency is the same as the input frequency until the shock wave is located downstream of the monitored position. It also must be noticed that when the shock wave approached from upstream of the monitoring position, the spectrum of the relatively low frequencies than the input frequency becomes large. On the other hand, in case of f=200Hz, although the dominant frequency is still the same as the input frequency, the low frequencies have much less spectrum power than that for f=100Hz. However, when the state of the flow at the monitoring position becomes supersonic due to the increase in the pressure ratio, the spectrum of all the frequencies is decreased, which are also deduced from the sudden reduction of the rms of the pressure fluctuation. On the whole all the experimental results show that quite small displacement of the piezo actuator at the throat causes the large shock wave displacement and the large pressure fluctuations, which suggest the promising and potential application of the actuator to the noise reduction and to the high powered speaker if all the characteristic of the behavior of the shock wave and the flow are fully understood.

T-2E-4. INFLUENCE OF THE EXPANSION RATE OF NOZZLE ON TWO-DIMENSIONAL SUBSONIC JET
S. Y. SHIN, *Kyungpook National University, Korea*, S. H. KIM, *Kyungpook National University, Korea*, Y. D. KWON, *Kyungpook National University, Korea*, S. B. KWON, *Kyungpook National University, Korea*, From the view points of frequent applications in diverse industries such as a mixing augmentation scheme, an air knife system and so on, two-dimensional turbulent free jets issuing from a symmetrical constant expansion rate nozzle are studied by a numerical analysis and experiment. In numerical analysis, we used the commercial code of Fluent 6.0, and two-dimensional Navier-Stokes equation with standard k-ε model is used as governing equation. To calculate the dynamic viscosity of working fluid, the Surtherland equation is used, and the working fluid is air. In the case of the same nozzle stagnation condition and system external configuration, the influences of the nozzle expansion rate on the jet structures, the velocity distributions, the potential core width and length and the growth of half widths are investigated. In the measuring of velocity, we used a pressure measuring system made with a stainless string of 0.8mm in outer diameter. As results, in the potential core region, we can't find exactly the similarities in velocity with the variations of expansion rate of nozzle, while the similarity of velocity in the fully developed region exists. And, for the same nozzle stagnation conditions, we can't find nearly the difference in potential core length with P. Furthermore, we can't find the difference of velocity gradients in y direction at the potential core regions of the same x. Finally, it is found that the decay angle of potential core θ regardless of nozzle expansion rate is around of 5.0°.

14:30 ~ 15:50 (Room 106)

Drops and Bubbles (II)

Session Chair : Prof. Mohammad Ali, BUET/Bangladesh

T-2F-1. MODELLING THE FORMATION OF A THERMAL SPRAY COATING USING A STOCHASTIC APPROACH
Mohammad P. FARD, Ali R. TEYMOURTASH and Ebrahim KAMALI,

Department of Mechanical Engineering, Ferdowsi University of Mashhad, Mashhad, Iran, Thermal spray coating is a particulate deposition process in which powders of a material are injected into a high temperature flame region where they are melted and propelled towards the surface of a substrate where individual molten particles impact, cool and solidify to form a deposit. This technology is used to produce coatings for wear, thermal, oxidation, and corrosion protection. In this paper, a 3-D stochastic model is used to simulate the coating morphology in a thermal spray coating process. Four main assumptions used in the stochastic model are: the spray droplets are non-interacting point particles; each droplet has a different size, velocity, and impact position; the spray is random; and the probability of obtaining a droplet occurrence at any instant is independent of other droplets occurring at other instants. It is assumed that the position of droplet impact follows the uniform distribution and the droplet specified diameter and velocity follow the Poisson distribution. The splashing and rebounding of droplets during the impact are not considered in this study. A set of rules are used to specify the final splat shape as a function of droplet impact conditions. These rules obtained from the literature are based on the numerical/analytical solution of the droplet spreading and solidification. Final splat shapes are characterized by dimensionless numbers known as Reynolds, Weber and Stefan. Due to temperature difference between droplet and substrate and thermal stresses after solidification, the edge of the splats is curled up. A new analytical model is used for this curl-up mechanism. The curl-up is assumed to be the sole reason for porosity formation. Simulations were performed for a small section of a substrate on which alumina droplets are sprayed. The computed thickness and porosity were in good agreement with those reported in the literature. In another simulation for aluminum droplets impinging on a steel substrate, the results for porosity were found in the range measured in experiments. The effect of substrate temperature on the porosity was also investigated. The results from both experiments and model show that by increasing the substrate temperature, the porosity increases. There were some discrepancies between the two results, however, that could be attributed to the existence of droplet splashing ignored in the model. The effect of spray materials on the coating porosity was also studied. The coating formed from the spray of alumina particles on a steel substrate had the lowest porosity and that of the nickel particle had the highest. The difference in porosity values for various materials can be attributed to droplet physical properties namely the surface tension and viscosity.

T-2F-2. A NUMERICAL MODEL FOR CALCULATION OF THE FORM AND VELOCITY OF LONG BUBBLES IN TUBE AT NEGLIGIBLE GRAVITY USING BOUNDARY ELEMENTS METHOD

HIEN Ha-Ngoc, *Institute of Mechanics, Hanoi, Vietnam,* The paper presents a numerical model for calculation the form and the velocity of long bubbles under micro-gravity conditions or in sub-millimeter tubes when surface tension dominates. To understand the role of surface tension, the numerical method is developed in frame of the inviscid theory. The bubble is assumed to be axi-symmetric and move at constant velocity with a prescribed velocity profile of liquid ahead the bubble. Then, the flow characteristics can be described by a Poisson equation for the Stockes stream function. An equation resulting from both Bernoulli equation and the pressure jump conditions at the interface is obtained and used for determining the bubble shape. The boundary elements method (BEM) was used to solve the problem in an iterative way to obtain simultaneously the flow characteristics, the bubble velocity and shape. The obtained results by the model are in good accordance with experimental results for the limit case of large bubble Reynolds number.

T-2F-3. FLOW INSIDE A DROPLET MOVING ON A FLAT SURFACE

A. HAYASHI, *Toyo University, Japan*, O. MOCHIZUKI, *Toyo University, Japan,* The purpose of this study is to investigate an entrainment mechanism of particles of dust into a droplet moving on a flat surface. This is useful for developing a way to clean a surface by using a droplet. The entrainment of dust into a droplet may be affected by conditions of a flow and surface of a wall. The flow inside a water droplet moving on a flat surface was visualized by starch particle. The droplet ran from left to right on the acrylic resin surface inclined 20 degrees. The speed of the droplet was 0.01 m/s. Its volume was 0.1×10^{-6} m^3. Its size was the length in the moving direction 10×10^{-3} m, width 5.4×10^{-3} m and height 2.5×10^{-3} m. The Reynolds number when assumed the width of the droplet representative dimensions was about 50. The dominant motion of particles observed in the side view picture was clockwise rotating flow. Particles near the wall were getting together, and were moving toward the rear along the center of the droplet. The flow patterns were topologically considered to know three-dimensional structures of the flow. There is a half vortex ring in the moving droplet. The half nodes are presented at both the front and rear positions on the wall in a droplet. The entrainment of starch particles dispersed on the surface of the wall. The droplet ran on the particles. It was found that the particles were captured only at the rear of the droplet. This is our important result.

T-2F-4. NUMERICAL SIMULATION OF FLOW INSTABILITIES DURING THE RISE OF A BUBBLE IN A VISCOUS LIQUID

Mohammad P. FARD, Mehran M. FARHANGI and Hossein MOIN, *Department of Mechanical Engineering, Ferdowsi University of Mashhad, Mashhad, Iran,* In this paper, the flow instabilities during the rise of a single bubble in a narrow vertical tube are studied using a transient 2D/axisymmetric model. These instabilities include the oscillation of the bubble shape and formation of a wake behind it. In the model, the Navier-Stokes equations in addition to an advection equation for liquid volume fraction are solved. A modified Volume-of-Fluid (VOF) technique based on Youngs' algorithm is used to track the liquid/gas interface. As a first step the model was subjected to several tests in order to validate its results. The results of simulations for terminal rise velocity and bubble shape are compared with those of the experiments. The results of the model, are predicted in the same region where observed by experiments. The results show that increasing the bubble diameter increases the rise velocity up to a certain limit after which the bubble starts to oscillate. In this regime, the rise velocity remains nearly constant. Further increase of the bubble diameter changes the deformation behavior to the spherical cap regime. Next we studied the flow instabilities that occur during the rise of a bubble in a narrow vertical tube. Driven by the buoyancy force, the bubble rises rapidly after its release. It is deformed from the initial spherical shape to the final bullet-like configuration. The bottom of the bubble moves rapidly upward and develops into a concave shape. It then rebounds downward immediately into a convex shape. This up-and-down oscillatory movement of the bubble bottom continues as the bubble rises with decreasing amplitude. The top of the bubble, on the contrary, remains a spherical cap shape with very little deformation as it ascends. Finally the effect of different parameters on the oscillatory behaviors of bubble velocity and shape are investigated.

14:30 ~ 15:50 (Room 107-108)

Computational Fluid Dynamics (V)

Session Chair : Prof. Y.-W. Lee, Pukyong Univ/Korea

T-2G-1. AN OIL SPILL MODEL FOR NORTHERN PERSIAN GULF WATERS

M. A. BADRI, A. R. AZIMIAN, *Department of Mechanical Engineering, Isfahan University of Technology, Iran,* In this paper, simulation of oil spill due to weathering and tidal currents in Persian Gulf is studied. Here, water current and wind-induced velocities are taken into account including many significant processes such as advection, surface spreading, evaporation, emulsification and dissolution. A grid with 339 points in the Persian Gulf have been generated. By means of WAve Model (WAM) and Cressman analysis on the whole grid, wind velocity and direction, wave height and wave period have been determined. Tidal constituents have been obtained from co-tidal charts and then tidal stream from tidal analysis program have been calculated to determine advection properties. Therefore, a portal have been provided to present simulation of the surface movement of the oil slick by Lagrangian approach for the northern part of the Persian Gulf waters. Sample simulations for oil spill are presented and the results are compared with the existing observed data. Comparison of wind and tide data and water surface level with the observed data and some other simulation results shows good agreement.

T-2G-2. NUMERICAL STUDY OF THE GAS FLOW THROUGH A CRICAL NOZZLE

S. MATSUO, *Saga University, Japan*, T. MITSUNAGA, *Saga University, Japan*, T. SETOGUCHI, *Saga University, Japan*, H. D. KIM, *Andong National University, Korea,* The critical nozzle is defined as a device to measure the mass flow with only the nozzle supply conditions, making use of the flow-choking phenomenon at the nozzle throat. The mass flowrate and critical pressure ratio are associated with the working gas consumption and the establishment of safe operation conditions of the critical nozzle. According to previous researches, the mass flowrate and critical pressure ratio are strong functions of Reynolds number. Some studies have shown that for high Reynolds numbers, based upon the velocity at the nozzle throat and the diameter of the nozzle throat, the discharge coefficient approaches unity, indicating that the one-dimensional theory is valid for the prediction

MODELLING THE FORMATION OF A THERMAL SPRAY COATING USING A STOCHASTIC APPROACH

Mohammad P. Fard *1, Ali R. Teymourtash *2 and Ebrahim Kamali *3

Department of Mechanical Engineering, Ferdowsi University of Mashhad, Mashhad, Iran
*1 mpfard@um.ac.ir *2 teymourtash@um.ac.ir *3 ebkamali@gmail.com

ABSTRACT: *In this paper, a 3-D stochastic model is presented to predict the coating thickness and porosity in a thermal spray coating process. The model is based on prescribed rules in calculating the splat size during the impact of individual droplets on the substrate. Due to thermal stresses, the edge of the splats is curled up. This mechanism was assumed to be the sole reason for the porosity formation. Simulations are performed for a small section of a substrate on which a thermal spray of alumina droplets and other material particles are examined. The computed thickness and porosity were found to be in good agreement with those reported in the literature.*
Keywords: Stochastic model, Thermal spray process, Coating formation, Coating porosity, Coating thickness.

1. INTRODUCTION

Thermal spray coating is a particulate deposition process in which powders of a material are injected into a high temperature flame region where they are melted and propelled towards the surface of a substrate where individual molten particles impact, cool and solidify to form a deposit. This technology is used to produce coatings for wear, thermal, oxidation, and corrosion protection. The coating quality obtained during thermal spraying depends greatly on the dynamics of flattening of the molten particles.

Inspection of a cross section through a thermal spray coating shows that it is built up of thin lamellae formed by flattened droplets that land on each other and fuse together. Closer examination shows that the coating is not fully dense and pores are found at the interface between splats. The presence of these pores may or may not be desirable, depending on the purpose of the coating so it is important to be able to produce the desired porosity by controlling the deposition process. Extensive theoretical, experimental and numerical studies have been reported in the literature to better control this process [1]. The ultimate goal of research efforts in this field is to establish predictive correlations between the processing parameters and the properties of the coatings. Modelling the build-up of a coating formation from the impact of individual droplets can only be performed using stochastic models less reported in the literature. Cirolini et al. [2] simulated coating deposition with a two dimensional stochastic model without considering the splat curl-up and used a set of complex rules to represent interaction between the splats. Ghafouri-Azar et al. [3] used a Monte-Carlo approach to model 3D coating formation assuming a normal distribution for the spray parameters. Belashchenko and Chernyak [4] used a stochastic approach to optimize thermal spray coatings. Their modeling results are in reasonable agreement with bond strength test data for the plasma-, arc-, and flame-spray processes as well as wear resistance data for arc-sprayed steel coatings. In this study, we developed a 3D stochastic model based on a Poisson distribution for the spray parameters and a new method for the splat curl-up to predict the microstructure and thickness of thermal spray coatings.

2. MATHEMATICAL DESCRIPTION

2.1. Stochastic Model

Four main assumptions used in the stochastic model are: spray droplets are non-interacting point particles; each droplet has a different size, velocity, and impact position; the spray is random; and the probability of obtaining a droplet occurrence at any instant is independent of other droplets occurring at other instants. It is also assumed that the impact position follows a uniform distribution and the droplet specified diameter and velocity follow a Poisson distribution with a user-specified mean (λ) and standard deviation (σ) as:

$$f(s;\lambda) = \frac{e^{-\lambda}\lambda^{k}}{s!}, \quad f_{Poisson}(s;\lambda) \approx f_{normal}(s;\delta=\lambda,\sigma^{2}=\lambda) \qquad (1)$$

where s is the stochastic parameter and δ is the mean value of normal distribution. The Poisson distribution will approach a normal distribution if n>100 and $(n\times p)$<10 where n is the number of occurrences and p is the probability of occurrence. A normal distribution was used by Ghafouri-Azar et al. [3] for the velocity and the logarithm of diameter. To generate random Poisson-distributed numbers for droplet parameters, we used the FORTRAN library written by Ahrens and Dieter [5].

2.2. Splat Deposition Model

A complete coating-formation model is complex due to time scales in the order of micro seconds and spatial scales ranging from a few micrometers to a few millimeters. In the model, we need to generally deal with: molten droplets at impact with their rebound, deposition, or splashing; a single particle flattening with the consideration of solidification before the end of flattening and possible splashing; a single splat cooling with nucleation at a hyper cooling temperature; and splat layering and deposition process. The present model considers only flattening with solidification without splashing and rebounding. The diameter and velocity of droplets and their impact location are introduced randomly as mentioned above. It is assumed that droplets impinge and spread on the substrate one after another. The model assumes that a spherical droplet spreads to form a cylindrical disc of diameter d_{max} as shown in Fig. 1. Thus, the effects of any droplet splashing and breakup are neglected.

In the model, a set of rules is used to specify the final splat shape as a function of droplet impact conditions. These rules, available in the literature [6,7], are obtained using a numerical/analytical solution of droplet spreading and solidification. The solution is based on the energy conservation law: the initial kinetic and potential (surface tension) energies of a droplet before impinging on the substrate are dissipated by the viscosity and surface deformation during the impact. Final splat shapes are characterized by dimensionless numbers known as Reynolds (Re), Weber (We) and Stefan (Ste). We used following relation for spread factor $\zeta_{\max}$ [3,6,7]

$$\xi_{\max} = \frac{d_{\max}}{D} = \sqrt{\frac{We + 12}{3(1-\cos\theta) + 4(We/\sqrt{\mathrm{Re}}) + We\sqrt{\frac{3}{4}\frac{Ste}{Pe}}}} \tag{2}$$

where D is diameter, θ contact angle, Pe=Re.Pr and

$$\mathrm{Re} = \frac{\rho V D}{\mu} \quad , \quad We = \frac{\rho V^2 D}{\gamma} \quad , \quad \mathrm{Pr} = \frac{C_l \mu}{k} \quad , \quad Ste = \frac{C_l (T_m - T_{w,i})}{H_f}$$

in which C_l is the specific heat, T_m melting point temperature, $T_{w,i}$ substrate temperature, and H_f heat of fusion. It is assumed that due to thermal stresses, the edge of the splat is curled up as seen in Fig. 1. The surface of the coating and the location of pores within it, are specified using a method known as the volume fraction [3,6]. During coating build-up, the mass conservation algorithm is enforced.

2.3. Splat Curl-up Model

The curl-up phenomenon at the edge of splats is one of the main sources of coating porosity. The degree of the curl-up is affected by several factors such as: stresses generated by mismatch of thermal expansion coefficients at the coating interface; surface tension of the liquid splat; surface roughness; and remelting. The mechanism of the curl-up is extremely complicated; therefore, few attempts have been made to qualify this phenomenon. Fukanuma [8] observed that most pores exist at the periphery of splats, starting at ~0.6 times the splat radius from its centre (Fig. 1). Ghafouri-Azar et al. [3] assumed in their model of thermal spray coating formation that all splats curl up at 0.6R from its centre. Sobolev and Guilemany [9] derived a set of analytical formula to describe the pressure distribution in a flattening droplet.

Curl-up location and magnitude depend on coating materials and impact conditions. Xue et al. [10] derived a simple analytical model to predict the curl-up angle as a function of impact parameters and material properties. Their model gives the curl up angle as [10]:

$$\theta = \arctan\left(\frac{xR\alpha\Delta T}{h_s}\right) \tag{3}$$

where x is the splat curl-up start position (0.6-0.7 times the splat radius), h_s the splat thickness, α the thermal expansion coefficient, ΔT the difference between droplet and substrate temperatures, and R the splat radius ($R=d_{max}/2$).

2.4. Porosity Calculation

Several possible sources of porosity in a coating have been defined including curling up of splats, incomplete filling of interstices during deposition [8], presence of unmelted particles in spray, satellite droplets formed by splat breakup at the time of impact, entrapment of gas between splats, and the presence of oxide layer on spray particle. These sources make the porosity sensitive to particle velocity, ambient gas pressure, particle diameter, and molten material viscosity. In this paper, only the effect of splat curl-up on porosity formation was considered. The curl-up was assumed to start at a radius equal to 60% of the splat radius with an angle specified by Equation 3. The porosity is defined as the fraction of the total volume of the coating occupied by voids [3,6]:

$$porosity = \frac{V_g}{V_g + V_m} \times 100 \tag{4}$$

where V_m and V_g are the volume occupied by solid material and voids respectively.

3. RESULTS

First, to examine the results of the stochastic model, the program is run several times for the same condition but with different random parameters. The results of these simulations are shown in Fig. 2. It is seen that the calculated porosity for 25 different runs (same case) is nearly the same. The obtained average thickness is 14.9171μm with a standard deviation of 0.4164. For all simulations presented in this paper, the average values of 25 runs with different random parameters were used as the final result.

The evolution of coating formation for a thermal spray process is shown in Fig. 3 where the cross-sectional areas of the final coating are also displayed. The variation of the coating thickness in the figure is shown with color range; pores within the coating can be clearly seen as holes in the cross sections. The surface roughness is also visible in the figure. This coating was formed by impinging 500 alumina droplets with a mean diameter of 40 μm and a mean velocity of 100 m/s on a steel substrate at 800 K. The program was run for 25 times; the average results obtained are: porosity=8%, maximum thickness=110 μm and average thickness=70 μm.

For a substrate temperature of 500 K, the results of the model for droplets of various materials with a mean velocity of 100 m/s and a mean diameter of 50 μm are shown in Fig. 4. The amount of x (Eq. 3) was assumed to be constant for all cases. The difference in the porosity values for different materials can be attributed to the droplet physical properties namely the surface tension and viscosity.

Finally to validate the model, the calculated results for a thermal spray process are compared with those of the measurements [1]. As seen from Table 1, a good agreement is obtained between calculated and measured values of the porosity. The results for another set of experiment are also compared with measurements [11]. As seen from Table 2, the calculated porosity for different cases with different substrate temperatures, are within the range reported in the experiments [11].

References

[1] Pawlowski L., *The science and engineering of thermal spray coatings*, 1st ed., John Wiley&Sons, 1995.
[2] Cirolini S., Harding H., and Jacucci G., "Computer Simulation of plasma-sprayed coatings deposition model", Surf. Coat. Technology, 48, 1991, 137-145.
[3] Ghafouri-Azar R., Mostaghimi J., Chandra S. and Charmchi M., "A stochastic model to simulate the formation of a thermal spray coating". J. of Thermal Spray Technology, 12(1), 2003, 53-69.
[4] Belashchenko V.E. and Chernyak Yu. B., "Stochastic approach to the modeling and optimization of thermal spray coating formation", J. of Thermal Spray Technology. 2 (2), 1993, 159-164.
[5] Ahrens J.H., and Dieter U., "Computer Generation of Poisson Deviates From Modified Normal Distributions", ACM Trans. Math. Software, 8(2), 1982.
[6] Pasandideh-Fard M., Bhola R., Chandra S. and Mostaghimi J., "Deposition of tin droplets on a steel plate: simulation and experiments". Int. J. of Heat and Mass Transfer, 41(19), 1998, 2929-2945.
[7] Mostaghimi J. and Chandra S., "Splat formation in plasma-spray coating process". Pure Applied. Chemistry, 74 (3), 2002, 441-445.
[8] Fukanuma H., "A Porosity Formation and Flattening Model of an Impinging Molten Particle in Thermal Spray Coatings", J. Thermal Spray Technology, 3(1), 1994, 33-44.
[9] Sobolev V.V. and Guilemany J. M., "Droplet-substrate impact interaction in thermal spraying", Journal of Material Letter, 28, 1996, 331-335.

[10] Xue M., Chandra S. and Mostaghimi J., "Investigation of splat curling up in thermal spray coatings", J. of Thermal spray Technology, 15 (4), 2006, 531-536.
[11] Abedini A., Pourmousa A., Chandra S. and Mostaghimi J., "Effect of substrate temperature on the properties of coatings and splats deposited by wire arc spraying", J. Surface and Technology, 201(6), 2006, 3350-3358.

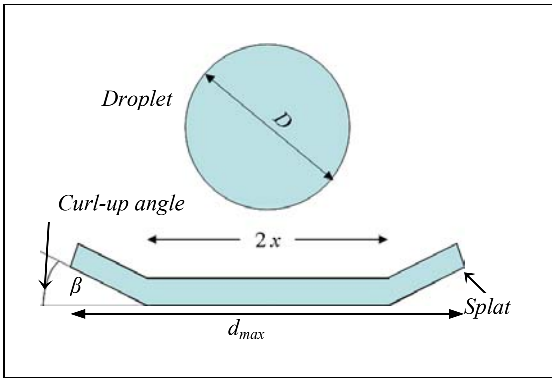

Fig. 1 A schematic of the droplet before the impact and the formed splat after the impact

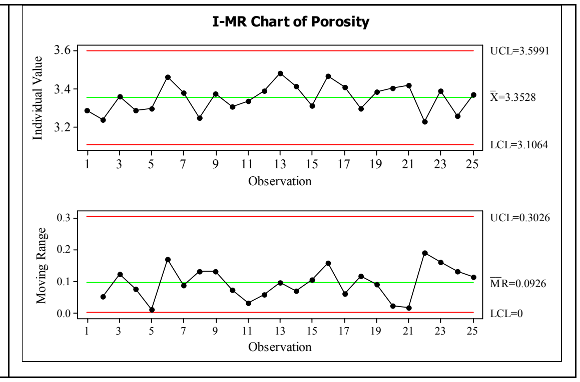

Fig. 2 The calculated porosity for 25 runs of the program for one case; the average porosity is 3.3538 with a standard deviation of 0.0734.

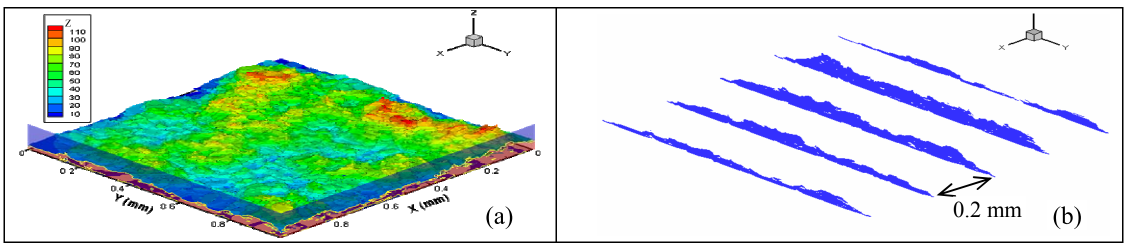

Fig. 3 Model results for a typical thermal spray process: a) the final coating topology and b) several cross-sectional areas. The porosity obtained in this case was 7%.

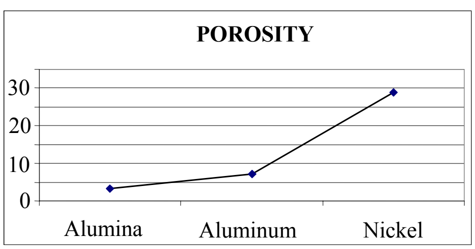

Fig. 4 The effect of spray materials on coating porosity

Table 1. A comparison between model predictions and measurements [1].

	Experiments	Model
Material	Alumina	Alumina
Mean diameter (μm)	-63+16	63
Mean velocity (m/s)	125	125
Porosity%	6.8	7.23
Ave. thickness (μm)	----	55.7
x	---	0.6

Table 2. Model results compared with measurements [11] for a thermal spray process (aluminum on stainless steel) with different conditions.

Substrate Temp. (ºC)	Porosity (%)			
	Case 1 (V_{av}=143±3 m/s)		Case 2 (V_{av}=109±2 m/s)	
	Measurements	Model Results	Measurements	Model Results
100	---	---	0.9 - 2.5	1.626
150	---	---	0.7 - 3.1	1.630
200	0.9 - 1.3	2.143	0.2 - 3.6	1.631
250	0.8 - 3.5	2.148	1.8 - 3.8	1.634
300	2.2 - 2.4	2.139	2.5 - 4.1	1.628